

This article was downloaded by:

On: 25 January 2011

Access details: *Access Details: Free Access*

Publisher *Taylor & Francis*

Informa Ltd Registered in England and Wales Registered Number: 1072954 Registered office: Mortimer House, 37-41 Mortimer Street, London W1T 3JH, UK



## Separation Science and Technology

Publication details, including instructions for authors and subscription information:

<http://www.informaworld.com/smpp/title~content=t713708471>

### Influence of Water Vapor on the Adsorption of VOCs on Lignin-Based Activated Carbons

José Rodríguez-Mirasol<sup>a</sup>; Jorge Bedia<sup>a</sup>; Tomás Cordero<sup>a</sup>; Juan J. Rodríguez<sup>b</sup>

<sup>a</sup> Chemical Engineering Department, School of Industrial Engineering, University of Málaga, Málaga, Spain <sup>b</sup> Chemical Engineering, University Autónoma of Madrid, Madrid, Spain

**To cite this Article** Rodríguez-Mirasol, José , Bedia, Jorge , Cordero, Tomás and Rodríguez, Juan J.(2005) 'Influence of Water Vapor on the Adsorption of VOCs on Lignin-Based Activated Carbons', *Separation Science and Technology*, 40: 15, 3113 – 3135

**To link to this Article:** DOI: 10.1080/01496390500385277

URL: <http://dx.doi.org/10.1080/01496390500385277>

## PLEASE SCROLL DOWN FOR ARTICLE

Full terms and conditions of use: <http://www.informaworld.com/terms-and-conditions-of-access.pdf>

This article may be used for research, teaching and private study purposes. Any substantial or systematic reproduction, re-distribution, re-selling, loan or sub-licensing, systematic supply or distribution in any form to anyone is expressly forbidden.

The publisher does not give any warranty express or implied or make any representation that the contents will be complete or accurate or up to date. The accuracy of any instructions, formulae and drug doses should be independently verified with primary sources. The publisher shall not be liable for any loss, actions, claims, proceedings, demand or costs or damages whatsoever or howsoever caused arising directly or indirectly in connection with or arising out of the use of this material.



## Influence of Water Vapor on the Adsorption of VOCs on Lignin-Based Activated Carbons

**José Rodríguez-Mirasol, Jorge Bedia, and Tomás Cordero**

Chemical Engineering Department, School of Industrial Engineering,  
University of Málaga, Málaga, Spain

**Juan J. Rodríguez**

Chemical Engineering, University Autónoma of Madrid, Madrid, Spain

**Abstract:** Activated carbons with a wide range of burn-off degrees obtained from Eucalyptus kraft lignin have been used to study the influence of the presence of water vapor on VOCs adsorption. The amount adsorbed and the rate of adsorption of both benzene and water vapor increase with activated carbon burn-off as a consequence of an increase of micropore volume, broadening of micropore size distribution and increasing development of meso- and macroporosity. Similar results were found for MEK and methanol. Benzene is only partially desorbed at the adsorption temperature and an appreciable amount of it remains in the carbon, most likely in the narrow micropores. On the contrary, water vapor is completely desorbed at the adsorption temperature and its adsorption profile clearly exhibits two steps with different adsorption rates, associated to water molecules adsorbed on the active sites given rise to cluster formation and further migration and filling of the micropores. Adsorption with mixtures of VOC and water vapor has been carried out. The total amount adsorbed by the carbon, near the equilibrium point, is higher than in the case of the stream containing only the VOC. The adsorption rates for the mixtures streams are similar to that for the corresponding streams containing only the VOC in the case of carbons with a well developed porous structure. However, the presence of water vapor increases the rate of adsorption on the activated carbons with narrower microporosity. Saturation of the activated carbon with water vapor prior to the adsorption of a mixture containing benzene and water vapor has shown little effect

Received 6 February 2005, Accepted 2 September 2005

Address correspondence to José Rodríguez-Mirasol, Chemical Engineering Department, School of Industrial Engineering, University of Málaga, Campus de El Ejido, 29013 Málaga, Spain. E-mail: mirasol@uma.es

on the amount of benzene adsorbed, suggesting that water and benzene molecules are adsorbed in different sites on the carbon surface.

**Keywords:** Adsorption, activated carbon, lignin, VOCs, benzene, methyl-ethyl-ketone, methanol, water vapor, polarity

## INTRODUCTION

Volatile organic compounds (VOCs) are among the most common and hazardous pollutants emitted by industrial processes dealing with thinners, degreasers, lubricants, polishes, paints, and liquid fuels (1–4). Occasional emissions like spills, leaks, or hazardous waste sites are also a significant source of VOCs (5–8).

Different techniques are used to control VOCs emissions from industrial sources, which involve both modifications of process equipment or raw materials, in order to decrease the impact of VOCs emissions and treatment of the effluent gas. The former would be, in many cases, the most desirable ones, but they are not always easy to implement. Among the latter group, destructive and recovery techniques can be found. Destructive methods cover thermal (9) and catalytic oxidation (10, 11), reverse flow reactor (12) and biofiltration (13). On the other hand, recovery methods include absorption (14), adsorption (either on zeolites (15–17) or activated carbons (18–24)), condensation (3) and membrane separation (25, 26).

For occasional emissions (leaks, spills, or hazardous waste sites), soil vapor extraction (SVE) is an *in situ* remediation technique widely used to remove volatile (and some semivolatile) organic compounds from the vadose zone. A major part of the cost of a SVE operation is the removal of VOCs from the effluent gas exiting from the extraction wells. Vapors extracted by the SVE process are typically treated using activated carbon, incineration, catalytic oxidation, or condensation (5–8).

Treatment of VOC polluted air streams by activated carbon adsorption, with subsequent solvent recovery or incineration, is gaining increasing importance as a technology that can perform at a satisfactory level for the strict limits required by the world-wide environmental regulations. The surface chemistry and porosity of activated carbons affect considerably the VOC adsorption process (27–30). Surface chemistry plays an important role in the case of polar VOCs, while porosity seems to be more significant when the adsorbed VOC is non-polar. On the other hand, boiling point, critical temperature, cross-sectional area, and dipole moment are the most important properties of VOC related to its adsorption on activated carbons (31).

Water vapor is one of the major impurities in atmospheric air and it is, in many cases, present in most air pollution control problems. The fact that the effluent gas streams to be treated in adsorption processes present virtually always water vapor may result in a very inefficient performance of the

activated carbon in VOCs removal. Capillary condensation of liquid water in the pores of the carbon may reduce the rate of diffusional mass transport. Competition between water molecules and VOC molecules for the adsorption site on the activated carbon may be expected as other possible source of difficulty for VOCs removal by activated carbon (32–36). The adsorption of water vapor by activated carbon is a phenomenon widely studied in the literature (37–44). It is generally accepted that water adsorption is governed by two main factors: surface chemistry and porosity. This process begins with the adsorption of water molecules in adsorption centers at low relative pressures. As relative pressure increases, water clusters formation takes place and, finally, when the clusters reach a critical size they have enough dispersive force to enter in the micropore and micropore filling occurs (41). However, a better knowledge of the effect of water vapor on the adsorption of VOCs on activated carbon is needed to be able to predict activated carbon performance.

The porous structure of the activated carbons depends, to a great extent, on the nature of their precursors. Lignin is the major waste of cellulose pulp mills, where its combustion plays a critical role in the recovery process of chemical reactants remaining in black liquors after wood pulping. However, many existing paper mills become chemical recovery limited if paper production is to be maximized by increasing production rate, due to the very expensive revamping of the evaporation train needed in this case. Therefore, among other considerations of chemical and environmental concern, the development of alternative ways for lignin processing is of potential interest for pulp mills.

In previous works, we have presented our results on the preparation and characterization of activated carbons by physical and chemical activation of lignin (45–47). These activated carbons showed a well developed porous structure with high apparent surface areas. In the present work, different activated carbons prepared by partial gasification with CO<sub>2</sub> of a kraft lignin char have been used to study the influence of activated carbon porosity, water vapor, and VOC polarity on the kinetic of adsorption of VOCs, using benzene, methyl-ethyl ketone (MEK) and methanol as target compounds.

## Experimental Procedures

### Activated Carbons Preparation

The lignin used in this study was obtained in a pilot plant from acid precipitation of kraft black liquors. Typical analyses have been reported elsewhere (45). Different activated carbons have been prepared from this lignin through carbonization at 623 K followed by CO<sub>2</sub>-partial gasification at 1123 K, using different reaction times to cover a wide range of burn-off or activation degree, from 20 to 80%. A more detailed description of the

activation procedure can be found elsewhere (45). The activated carbons obtained have been designated by the letter H followed by a number that represents the burn-off or activation degree (%).

#### Porous Structure Characterization

The porous structure of the activated carbons has been characterized by  $N_2$  adsorption-desorption isotherms at 77 K and  $CO_2$  adsorption isotherms at 273 K, both using an Autosorb-1 system (Quantachrome). The samples were previously outgassed at 548 K for 12 hours to a residual pressure lower than  $10^{-3}$  Torr. Mercury porosimetry measurements were also carried out using a Carlo Erba Porosimeter 4000.

#### VOC Adsorption-Desorption

Adsorption of three VOCs with different polarity, benzene, methyl ethyl ketone (MEK) and methanol, at partial pressures ranging from 0.6 to 13 kPa, in dried and wet air streams, was carried out gravimetrically in a thermobalance analyzer (CI electronics) connected to a personal computer. The water vapor partial pressures ranged from 0.2 to 2.3 kPa. The adsorption experiments were performed at atmospheric pressure and 293 K, using approximately 10 mg of carbon sample, for a total flow rate of  $100\text{ cm}^3/\text{min}$ . Mass flow controllers (5800 Brooks, Fisher Rosemount) of various ranges were used to control the flow rates. Different air streams were conducted through vapor saturators, containing VOC or/and water, in order to obtain the desired VOC, water vapor or VOC/water vapor inlet concentration. Desorption experiments were also performed in the thermogravimetric system at the adsorption temperature under dry air stream ( $100\text{ cm}^3/\text{min}$ ) and, in some cases, the VOCs in the outlet stream were analyzed by mass spectrometry (QS 200, Balzers). Prior to the adsorption experiments the carbon samples were outgassed in vacuum ( $<10^3$  Torr) at 353 K during 12 hours. A liquid-phase specific volume of  $1.151\text{ cm}^3/\text{g}$  has been used in calculations for benzene. Due to the toxicity of the VOCs used precautions have been taken during the experimental procedures.

#### Chemical Vapor Infiltration

(CVI) of H-54 sample with pyrolytic carbon was carried out in a tubular horizontal laboratory furnace at 973 K and atmospheric pressure, using benzene (2%v in a stream of He) as pyrolytic carbon precursor, with a total flow rate of  $200\text{ cm}^3/\text{min}$ . The new sample obtained after the CVI process was identified as CVI-H-54.

## RESULTS AND DISCUSSION

### Activated Carbons Characterization

$N_2$  adsorption-desorption (77 K) and  $CO_2$  adsorption (273 K) isotherms and mercury porosimetry of the activated carbons used in this study have been reported in a previous paper (45). Figure 1 summarizes the evolution of the porous structure of the carbons as burn-off values increase. As activation proceeds an increase of micropore volume and widening of micropore size distribution takes place, as indicated by the higher differences observed between the micropore volume obtained from  $N_2$  and  $CO_2$  adsorption isotherms. The contribution of mesoporosity becomes relevant at intermediate burn-off levels, H-54 presents much higher value of mesopore volume than H-21. The development of macroporosity is achieved at higher activation degree, as suggested by the important increase in macropore volume of carbon H-77 compared to H-64.

### Benzene Adsorption

Benzene adsorption isotherms at 293 K are reported in Fig. 2. The amount of benzene adsorbed increases with carbon burn-off, as a consequence of the increase in the micropore volume, broadening of micropore size distribution, and development of meso- and macroporosity (48). Benzene adsorption isotherms confirm the results inferred from  $N_2$  adsorption. H-21 activated carbon adsorbs benzene mainly at low relative pressures, where micropore

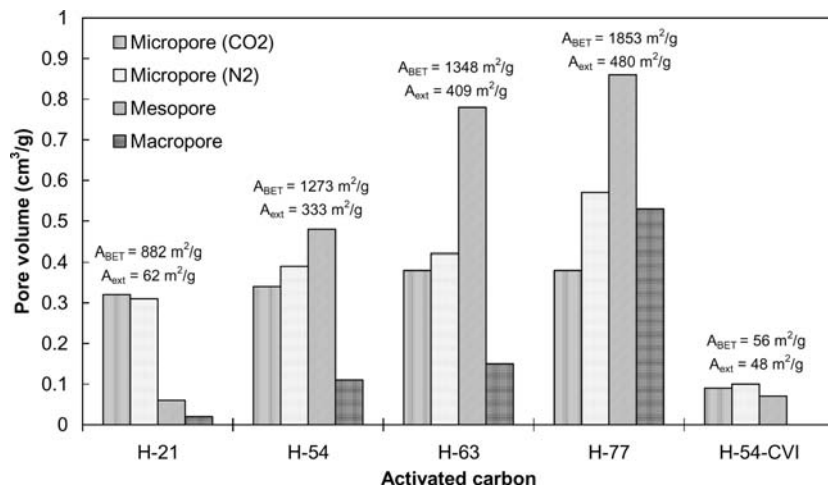


**Figure 1.** Evolution of the porous structure of different activated carbons.  $A_{BET}$ : BET apparent surface area;  $A_{ext}$ : External surface area.

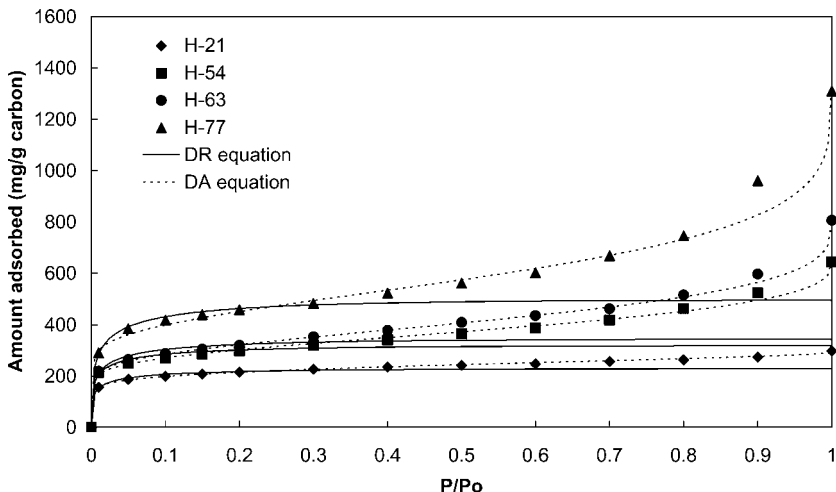


**Figure 2.** Benzene adsorption isotherms at 293 K for different activated carbons:  $\blacklozenge$  H-21;  $\blacksquare$  H-54;  $\bullet$  H-63;  $\blacktriangle$  H-77; solid line: DR equation; dashed line: DA equation.

volume filling takes place. The isotherm for this carbon exhibits an almost horizontal plateau, starting at very low relative pressure, which indicates very little contribution of meso- and macroporosity. Increasing the activation degree leads to a substantial increase of benzene adsorption at low relative pressures, i.e., in micropores. The isotherms exhibit a more open knee which extends up to increasingly higher relative pressures as burn-off increases, indicating a gradual widening of the microporosity. The higher slope of the plateau-like region of the isotherms of the activated carbons with higher burn-off indicates the progressive contribution of meso- and macroporosity to benzene adsorption as activation proceeds.

Benzene adsorption isotherms have been fitted by the Dubinin-Radushkevich (DR) equation, based on Polanyi's theory, which was developed to describe physical adsorption on microporous carbons (49):

$$W = W_0 \cdot \exp[-(A/\beta E_0)^2]$$

where  $W$  represents the mass of adsorptive adsorbed per gram of adsorbent at temperature  $T$  and relative pressure  $P/P_0$ ,  $W_0$  is the total amount of benzene adsorbed in the micropores,  $\beta$  is the affinity coefficient of the adsorptive ( $\beta = 1$  for benzene),  $E_0$  is the characteristic adsorption energy and  $A$  is the differential molar work that can be expressed as follow:

$$A = RT \ln(P_0/P)$$

where  $P$  represents the partial pressure of the adsorptive and  $P_0$  is its saturation vapor pressure at temperature  $T$ .

The DR model fits the benzene adsorption isotherms only at low relative pressures (solid lines in Fig. 2), where benzene adsorption takes place in micropores. Table 1 reports the values of  $W_0$  and  $E_0$  parameters obtained from the fitting of the benzene isotherms of the different activated carbons with the DR equation. The value of  $W_0$  increases with activation degree and agrees very well with the corresponding value of micropore volume obtained from the  $N_2$  isotherms (see Fig. 1). This result indicates that benzene fills not only the narrow micropores but also the wider ones of the different carbons.  $E_0$  is a function of the micropore size distribution of the adsorbent and decreases at increasing burn-off, in agreement with a wider pore size distribution (50). The Dubinin-Astakhov (DA) equation (51), a more general form of the DR one, has also been used for the modeling of the benzene isotherms:

$$W = W_0 \cdot \exp[-(A/\beta E_0)^n]$$

This equation presents a new parameter, the exponent  $n$ , which is related to the average size of micropores and the micropore size distribution. The DA model fits well the benzene adsorption isotherms of the different activated carbons in the whole range of relative pressure, as can be observed from Fig. 2 (dashed line). The parameters resulting from the fitting,  $E_0$ ,  $n$  and  $W_0$ , are shown also in Table 1. The values of  $W_0$  and  $E_0$  follow a similar trend as those obtained from the DR equation, i.e.,  $W_0$  increases and  $E_0$  decreases with burn-off, due to the already mentioned development of porosity and to the weakening of the potential overlap between pore walls, respectively (49). The values of  $n$  obtained from the DA equation decrease with activation degree and are relatively low with respect to those found in the literature (49, 52).  $n$  values approaching 3 are frequently found for adsorbents with narrow micropores, while values of  $n$  around 1 describe solids with a wide range of pore size (53). Terzyk et al. (54), in a theoretical study, observed that lowering the parameters  $n$  and  $E_0$  of the DA equation leads to a change in the micropores adsorption mechanism, from primary to simultaneous primary and secondary micropore filling. They found a bimodal micropore size distribution with

**Table 1.** Values of the parameters obtained from the fitting of the benzene isotherms of the different activated carbons with the Dubinin-Raduskevich (DR) and Dubinin-Astakhov (DA) equations

Dubinin-Raduskevich (DR)				Dubinin-Astakhov (DA)		
$E_0$ (kJ/mol)	$W_0$ (mg/g CA)	$V$ (cm <sup>3</sup> /g)	$n$	$E_0$ (kJ/mol)	$W_0$ (mg/g CA)	$V$ (cm <sup>3</sup> /g)
H-21	17.70	228	0.262	0.65	24.13	291
H-54	16.92	318	0.366	0.38	7.87	649
H-63	16.02	343	0.395	0.35	5.05	803
H-77	15.08	495	0.570	0.30	2.97	1336

pore size of around 0.7 and 1.2 nm for  $E_0$  and  $n$  values of 10 kJ/mol and 0.5, respectively, and the presence of mesopores. The presence of a wide micropore size distribution and mesopores in the activated carbons studied in this work would explain the much higher values of  $W_0$  found with the DA model than with the DR one, very close to the total micropore plus narrow mesopore volume obtained from the  $N_2$  adsorption isotherm (see Fig. 1), and the low values obtained for the  $n$  parameter.

Figure 3 a shows the amount of benzene adsorbed at 293 K and 50% relative pressure as a function of time for the different activated carbons.

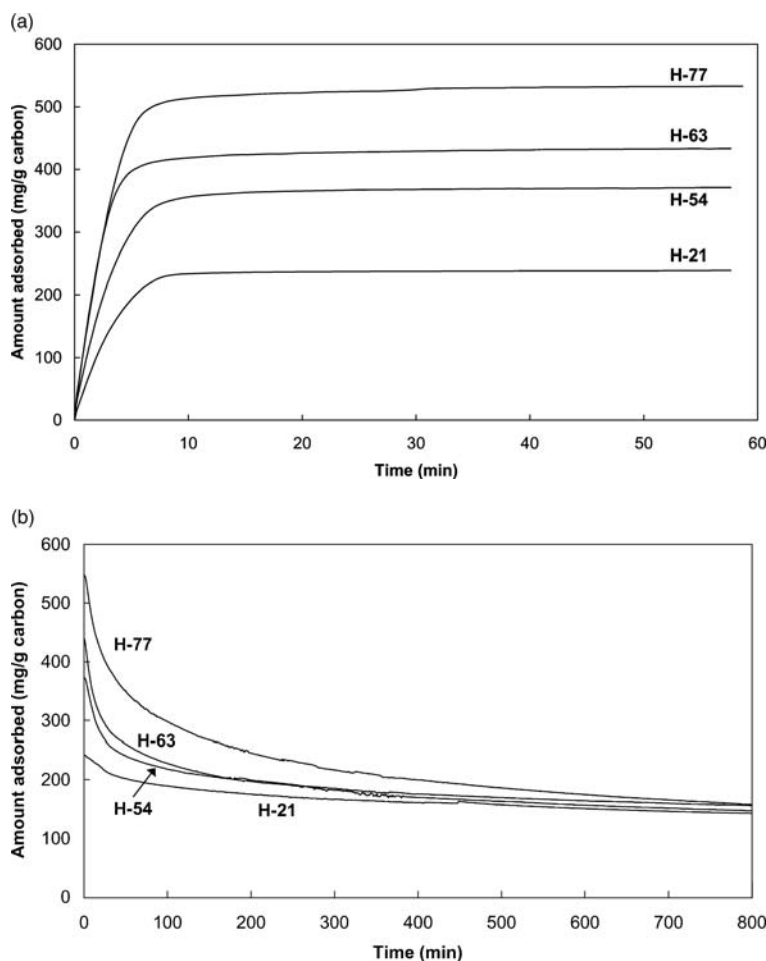


**Figure 3.** (a) Amount of benzene adsorbed as a function of time for different activated carbons at 293 K and 0.5 benzene relative pressure. (b) Amount of benzene adsorbed as a function of time at 293 K in a dry-air stream for different activated carbons previously loaded with benzene at 293 K and 0.5 relative pressure.

The adsorption rate and the total amount of benzene adsorbed increase with carbon burn-off as a consequence of the broadening of the pore size distribution and the increasing development of porosity upon activation. Figure 3b represents the benzene desorption at 293 K in a dry air stream for the activated carbons previously adsorbed at the same temperature and 0.5 benzene relative pressure. It can be observed that the desorption time is longer than the adsorption one. A similar behavior has been reported for adsorption of butane on a microporous activated carbon (55, 56).

All these curves present initially a relatively fast desorption that is followed by a second region where the desorption rate decreases notably. The first region may be related to desorption from the wider micropores. In fact, the rate of desorption for this region on H-21 carbon, which contains a much narrower microporous structure, is lower than for the other carbons. The second region could be due to a more difficult desorption of benzene from narrow micropores. Actually, benzene is only partially desorbed at the adsorption temperature, with an appreciable amount of it, approximately 170 mg/g, remaining adsorbed on the different carbons, most likely in the narrow micropores. Similar results were found for different benzene relative pressures. The amount retained in the different carbons after desorption at the adsorption temperature represents a fraction of about 50% of the micropore volume calculated from the  $\text{CO}_2$  adsorption isotherms (see Fig. 1). This result suggests that all these carbons present a similar volume of very narrow micropores, probably produced during the lignin carbonization step (45), where the adsorption energy of benzene may be greatly enhanced by the superposition of the adsorption potentials of the opposite micropore walls (38), retaining the benzene very strongly adsorbed. Nevertheless, the benzene thus retained can be easily desorbed by heating the carbons at 313 K. Huang et al. (57) reported shorter desorption time than adsorption one for benzene adsorption/desorption on a microporous carbon fibre, with benzene totally removed during the desorption step. However, the desorption experiments were carried out at 393 K, 100 K higher than the adsorption ones, a temperature high enough to desorb benzene from the narrower micropores of the fibre.

### Water Adsorption

Water adsorption isotherms for the different carbons are shown in Fig. 4. The amount of water adsorbed increases with the activation degree, as the micro- and mesoporous structure is developed. The isotherms are of type V, where the filling of the main pore volume of the carbons with water vapor occurs at high relative pressures. Three different sections can be observed, which are related to changes in the adsorption process. Up to relative pressures approaching 0.3 chemisorption of water molecules on adsorption sites, such as oxygen surface group or inorganic impurities, takes place. From

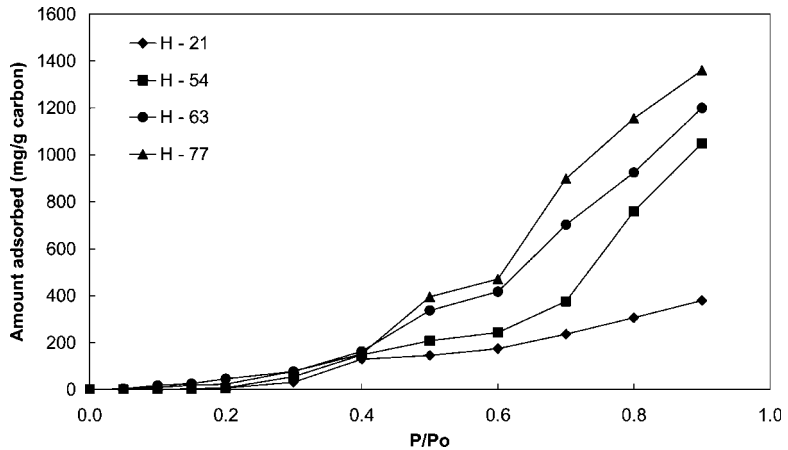


**Figure 4.** Water vapor adsorption isotherms at 293 K for different activated carbons: ◆ H-21; ■ H-54; ▲ H-63; ● H-77.

values of 0.3 to 0.6 further water adsorption occurs on top of the chemisorbed water molecules via formation of hydrogen bonds, resulting in the growth of water clusters around the chemisorption sites (38, 41). As the water pressure is increased in the gas phase the clusters reach a critical size, attaining a sufficient dispersive energy to enter and fill the micropores (41, 58). At high relative pressures capillary condensation in meso- and macropores begins (59).

Figure 5 shows the water adsorption kinetics at 293 K and a water relative pressure value of 0.8 for the different activated carbons. The adsorption of

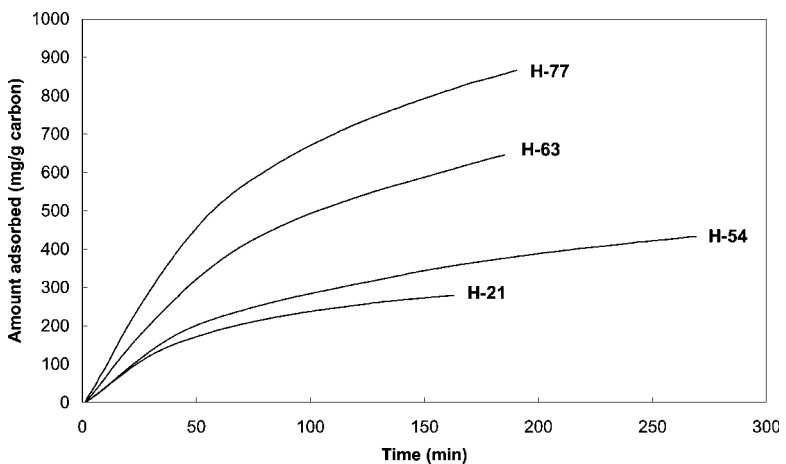


**Figure 5.** Amount of water vapor adsorbed as a function of time for different activated carbons at 293 K and 0.8 water vapor relative pressure.

water vapor proceeds initially at a high and constant rate and after a certain amount of water is adsorbed the rate of adsorption substantially decreases, progressively. The initial high rate step may be related with the chemisorption of water molecules on adsorption sites (oxygen surface group and impurities) and the growth of water clusters around these sites, whereas the second step, less rapid, can be associated to the filling of micropores and condensation on meso- and macropores. The diffusion of the water molecules through the very narrow micropores of the lower burn-off H-21 and H-54 carbons may limit the chemisorption and cluster enlargement process, reducing significantly the rate of the initial adsorption step of these carbons with respect to the other ones.

The diffusion kinetics of benzene and water vapor on the different activated carbons has been analyzed using an approximation of the Fickian diffusion in a spherical particle for small times (60):

$$W_t/W_\infty = 6D^{1/2}t^{1/2}/\pi^{1/2}r_0$$

where  $W_t$  is the mass uptake at time  $t$ ,  $W_\infty$  the mass uptake at equilibrium,  $t$  the adsorption time,  $D$  the diffusion coefficient, and  $r_0$  the particle radius. A plot  $W_t/W_0$  versus  $t^{1/2}$  will have a slope of  $6D^{1/2}/\pi^{1/2}r_0$  from which the diffusional parameter,  $D/r_0^2$ , can be calculated. Table 2 compares the diffusional parameter values for adsorption of benzene at 0.2 relative pressure and water vapor at 0.8 relative pressure. The diffusional parameter for benzene is considerably greater than that for water and in both cases increases clearly with activation degree, although this increase is more significant for benzene than for water. This suggests that the rate of benzene adsorption is favored by the widening of the micropores and the development of meso- and microporosity. However, although this may also be important, in the case of water vapor the step governing the rate of adsorption seems to be the chemisorption of water molecules on the adsorption sites and the following cluster formation.

Desorption profiles at 293 K in a dry air stream for H-54, H-63 and H-77 carbons previously adsorbed with water vapor at 293 K and 0.8 relative

**Table 2.** Values of the diffusional parameter ( $D/r_0^2$ ) for adsorption of benzene at 0.2 relative pressure and water vapor at 0.8 relative pressure on different activated carbons at 293 K.

Sample	$D/r_0^2 [10^{-6} \cdot \text{s}]$	
	Benzene $P/P_0 = 0.2$	Water vapor $P/P_0 = 0.8$
H-21	108.16	6.76
H-54	151.29	8.41
H-63	210.25	7.84
H-77	349.69	9.61

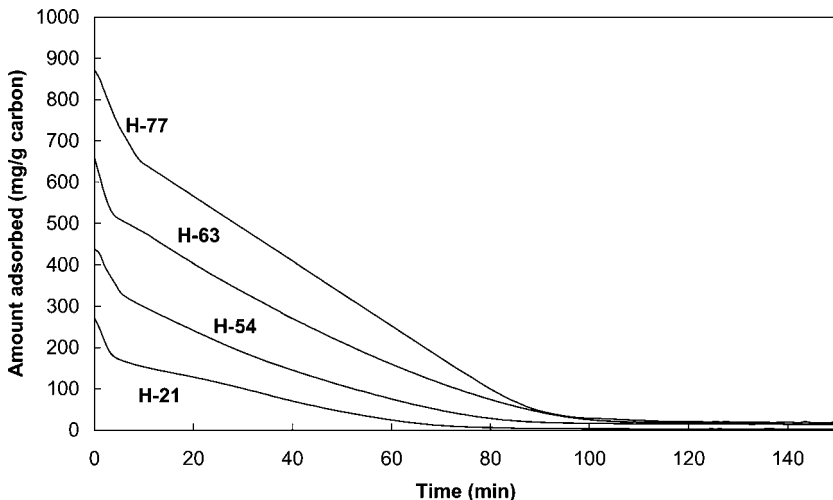


**Figure 6.** Amount of water vapor adsorbed during the desorption cycle as a function of time at 293 K in a dry-air stream for different activated carbons previously loaded with water vapor at 293 K and 0.8 relative pressure.

pressure are depicted in Fig. 6. Water vapor, unlike benzene, is desorbed completely at the adsorption temperature, as a result, probably, of a less effective enhancement of the adsorption potential for water molecule due to superposition of the fields of opposite pore walls in the narrow micropores (38). The desorption profiles clearly exhibit two steps with different desorption rates, probably as a consequence of the reversible processes derived from the two different adsorption steps mentioned above.

### Influence of Water Vapor on Benzene Adsorption

In order to study the efficiency of these lignin-based activated carbons for VOCs removal from industrial or hazardous waste sites off-gas streams containing water vapor, the influence of water vapor on the adsorption of benzene is analyzed in this section for the different activated carbons. A stream with a low concentration of benzene ( $P/P_0 = 0.2$ ) and almost saturated with water vapor (80% relative humidity) has been chosen. Figure 7 represents the kinetics of adsorption and desorption at 293 K for H-63 carbon with this inlet mixture stream, to which corresponds water and benzene partial pressures of 1.87 and 2.06 kPa, respectively. For the sake of comparison the corresponding curves for streams containing only water and only benzene at the same concentrations than in the mixture have been included in the figure. Desorption was, in all cases, carried out at the adsorption temperature in a dry water- and benzene-free air stream. It has to

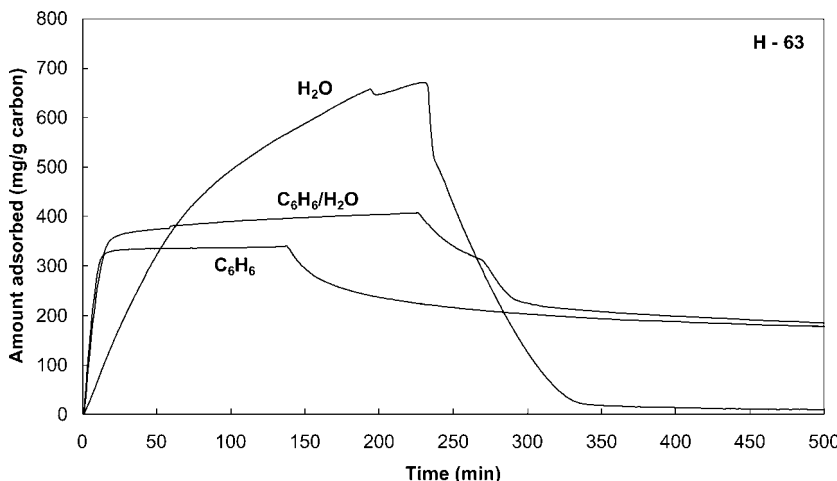


**Figure 7.** Amount adsorbed during the adsorption/desorption cycle as a function of time on H-63 activated carbon at 293 K with inlet streams containing benzene ( $P/P_0 = 0.2$ ), water vapor ( $P/P_0 = 0.8$ ) and a mixture of benzene/water vapor at the same relative pressures, respectively.

be noted that in the experiments with mixture of benzene and water vapor the “amount adsorbed” represents the total mass adsorbed on the carbons.

The initial adsorption step for the stream containing a mixture of benzene and water vapor on H-63 carbon takes place at a similar rate as that for the stream containing only benzene. It can also be observed that a slightly higher amount is adsorbed during this step when water is present. When the feeding stream contains only benzene the equilibrium of adsorption is reached rapidly after the initial adsorption step. However, a second step with a lower adsorption rate can be observed in the case that the mixture stream is supplied to the system, resulting in a higher total amount adsorbed by this carbon near the equilibrium. The increase in the amount adsorbed in the second and slower adsorption step could be associated to the adsorption of water on the free micro- and mesopore surface left by benzene molecules.

The desorption profile for the case of the inlet stream containing a benzene/water vapor mixture exhibits, at least in three steps and clearly differentiated and shows that a significant amount of adsorbate, similar to the amount of benzene retained by the carbon in the case of a stream containing only benzene, remains on the carbon at the desorption temperature. The evolution of the desorption products have been analyzed using a mass spectrometer. The first step is due to the desorption of benzene. The rate of desorption of this region is similar to that of the initial desorption step when water was not present, which suggests that benzene is likely been desorbed from the wider micropores and/or mesopores. The second step, with a higher rate, corresponds to desorption of water. The similarity between the rate of this second step and that of the

second region of the desorption profile for water adsorption in absence of benzene, suggests that this step is related to desorption of water clusters and water molecules chemisorbed on adsorption centers. The low desorption rate of the third desorption step corresponds to benzene and compares quite well with the slower desorption observed in the curve for the case in which only benzene was supplied to the system. This indicates that benzene has been removed from the narrower micropores in the last step of desorption. The total amount of benzene desorbed (during the first and third desorption steps) together with the amount retained in H-63 carbon after desorption equals, closely, the total mass of benzene adsorbed on this activated carbon when water is not present. It is also interesting to point out that only a small amount of water is adsorbed for a long adsorption time, when a mixture of benzene and water vapor is fed to the system. This result indicates that the presence of water in the inlet stream does not appreciably affect the rate of adsorption and the total amount of benzene adsorbed on H-63 carbon. It seems that in the presence of water vapor benzene occupies rapidly a large part of the micropore volume, impeding partially the slow adsorption of water vapor on the surface of these pores. It is noteworthy that the presence of water vapor hastens the adsorption and slightly increases the total amount of benzene on the activated carbons with narrower microporosity, as it is the case for H-54 and H-21 carbons (shown in Fig. 8).

Figure 9 shows the kinetics of adsorption of a mixture of water vapor and benzene at 293 K on H-54 carbon previously adsorbed with water vapor. Initially, adsorption of water vapor at 0.8 relative pressure on H-54 was

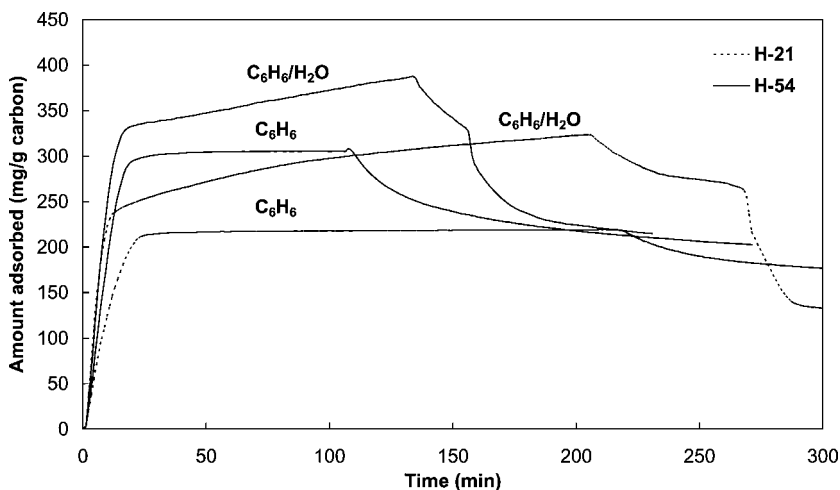


**Figure 8.** Amount adsorbed during the adsorption/desorption cycle as a function of time on H-21 and H-54 activated carbons at 293 K with inlet streams containing benzene ( $P/P_0 = 0.2$ ), and a mixture of benzene/water vapor (0.2/0.8 relative pressures for benzene and water vapor, respectively).

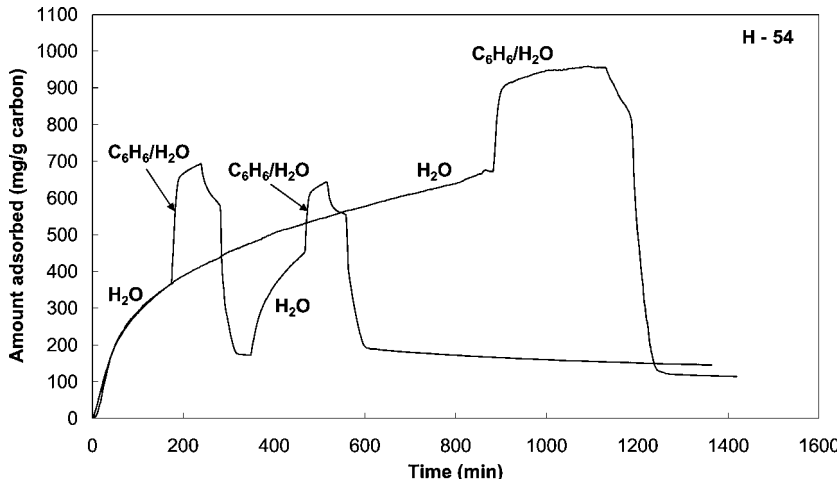


**Figure 9.** Amount adsorbed during different adsorption/desorption cycles with an inlet stream containing a benzene/water vapor (0.2/0.8 relative pressures for benzene and water vapor, respectively) mixture as a function of time on H-54 activated carbon previously loaded with water vapor at 0.8 relative pressure. Adsorption and desorption temperatures: 293 K.

carried out. After approximately 180 min of water vapor adsorption, a flow with the benzene/water vapor mixture was passed through the sample. A fast adsorption takes place initially, followed by a slower adsorption. The rapid adsorption presents a diffusional parameter value of  $204.5 \times 10^{-6} \text{ s}^{-1}$ , slightly higher than the corresponding value obtained for a stream containing only benzene (Table 2). At a time of about 230 min desorption begins, showing a similar profile as that observed for the experiment in which no pre-adsorption of water vapor took place. The only apparent difference appears in the second step, corresponding to water desorption, where a higher mass decrease is observed. The mass desorbed during the first and third desorption steps plus that retained by the carbon matches the mass gained during the adsorption experiment for H-54 carbon with an inlet stream containing only benzene (Fig. 8), which suggests that preloaded water on the carbon does not affect the adsorption of benzene. After the third desorption step, where once more a certain amount of benzene was retained in the carbon, the experiment was repeated, with a very similar result.

In a different experiment, preloading of water on the same carbon close to its equilibrium point was carried out previously to introduce the water vapor/benzene mixture into the system. The results show a similar behavior that those obtained in the previous experiments and are compared in Fig. 9. The rapid adsorption step observed after the introduction of the mixture presents a diffusional parameter value of  $166.4 \times 10^{-6} \text{ s}^{-1}$ , lower than those obtained for the

experiment in which a lower amount of water was preloaded, but still higher than that calculated for the stream containing only benzene. Now the mass desorbed during the first step is slightly higher, the third desorption step is faster and the amount retained in the carbon somewhat lower, suggesting that filling of a few fractions of micropore volume by water has taken place. Nevertheless, still about 260 mg of benzene per g of carbon have been adsorbed after loading the carbon with water vapor near the equilibrium, which represents about 85% of the benzene adsorption capacity of the carbon.

It seems also that water vapor does not fill the narrower micropores where benzene can penetrate. In order to study this possibility, H-54 sample was infiltrated with pyrolytic carbon by cracking of benzene at 973 K and atmospheric pressure. The porous structure of CVI-H-54, the sample obtained after the chemical vapor infiltration process, is summarized in Fig. 1. The micropore volumes both obtained from the  $N_2$  and the  $CO_2$  adsorption isotherms and the mesopore volume have been drastically reduced and similar BET and external surface areas values are obtained with both adsorbates, indicating that large micropore and mesopore volume have been blocked since all the area measured is now an external surface (61, 62). Nevertheless, a micropore volume of  $0.1\text{ cm}^3/\text{g}$  measured with  $CO_2$  is present in the carbon, most likely due to formation of narrow micropores by reduction of the narrower mesopores (63).

Figure 10 represents the amount adsorbed and desorbed on CVI-H-54 sample at 293 K for inlet streams containing only benzene, a mixture of benzene/water vapor and the same mixture but after previous loading of

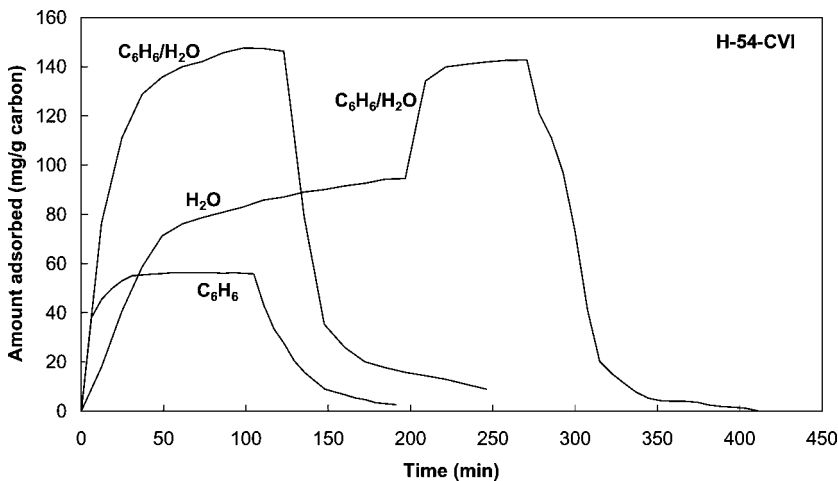


**Figure 10.** Amount adsorbed during adsorption/desorption cycles with inlet streams containing benzene ( $P/P_0 = 0.2$ ) and a benzene/water vapor ( $0.2/0.8$  relative pressures for benzene and water vapor, respectively) mixture as a function of time on H-54-CVI carbon and with the same mixture but on H-54-CVI carbon previously loaded with water vapor at  $0.8$  relative pressure. Adsorption and desorption temperatures:  $293\text{ K}$ .

the carbon sample with water vapor, close to the equilibrium point. A large reduction of the amount adsorbed and a complete desorption can be observed in all the cases. The reduction in the amount of water vapor adsorbed is very much higher than for the case of benzene. Despite the micro- and mesopore volume reduction, the pyrolytic carbon deposited on the carbon surface must block the adsorption sites available to chemisorb water molecules. Almost the same mass was gained for the experiments carried out with the water vapor/benzene mixture with and without water preloading, although a different desorption behavior seems to apply. Three desorption steps appear in the case of water vapor preloading, which can be explained as in the experiment represented in Fig. 7. However, only two can be observed in the case that water vapor was not preloaded, corresponding the first one to water vapor from the wider micropores and the second to benzene from the narrow ones. The amount of benzene adsorbed in the sample saturated with water is somewhat lower than that adsorbed for the inlet stream containing only benzene. These results seem to indicate that benzene adsorbs rapidly in the narrow micropores still available in the sample, where water vapor can only slightly penetrate if it is preloaded in the carbon.

### Influence of the VOC Polarity

Adsorption-desorption experiments with MEK and methanol were also carried out to learn about the influence of the VOC polarity. Figures 11a and b represent the amount of benzene, MEK and methanol adsorbed on activated carbons H-54 and H-77, respectively, at 293 K and 0.2 VOCs relative pressure. As well as for benzene, the amount adsorbed and the adsorption rate for MEK and methanol increase with burn-off. Besides, the mass adsorbed and the rate of adsorption is higher for benzene than for MEK and higher for MEK than for methanol, in spite of the higher partial pressure of methanol (2.53 kPa) than of MEK and benzene (2.18 and 2.06 kPa, respectively). Nevertheless, it has to be pointing out that the volume of methanol adsorbed is higher than that of MEK and benzene. It is also interesting to note that a certain amount of MEK, almost the same as benzene, is retained in the carbons. However, methanol, like water vapor, is completely desorbed.

Adsorption of benzene, a non polar VOC, is physical, involving unspecific interactions (e.g., dispersion attractive and short-range repulsion forces). The rate of adsorption for the polar VOC studied decreases with VOC polarity. The presence of the ketone group confers some polarity to the molecule of MEK (2.76 D). Methanol molecule exhibits an even higher polarity due to the presence of OH group (2.87 D). The adsorption of polar molecules on microporous carbons involves chemisorption or strong specific interactions between the adsorbate and the carbon surface sites, especially at low relative pressures. The OH group provides the methanol molecule the capacity to form hydrogen bonds (64, 65), as it occurs with

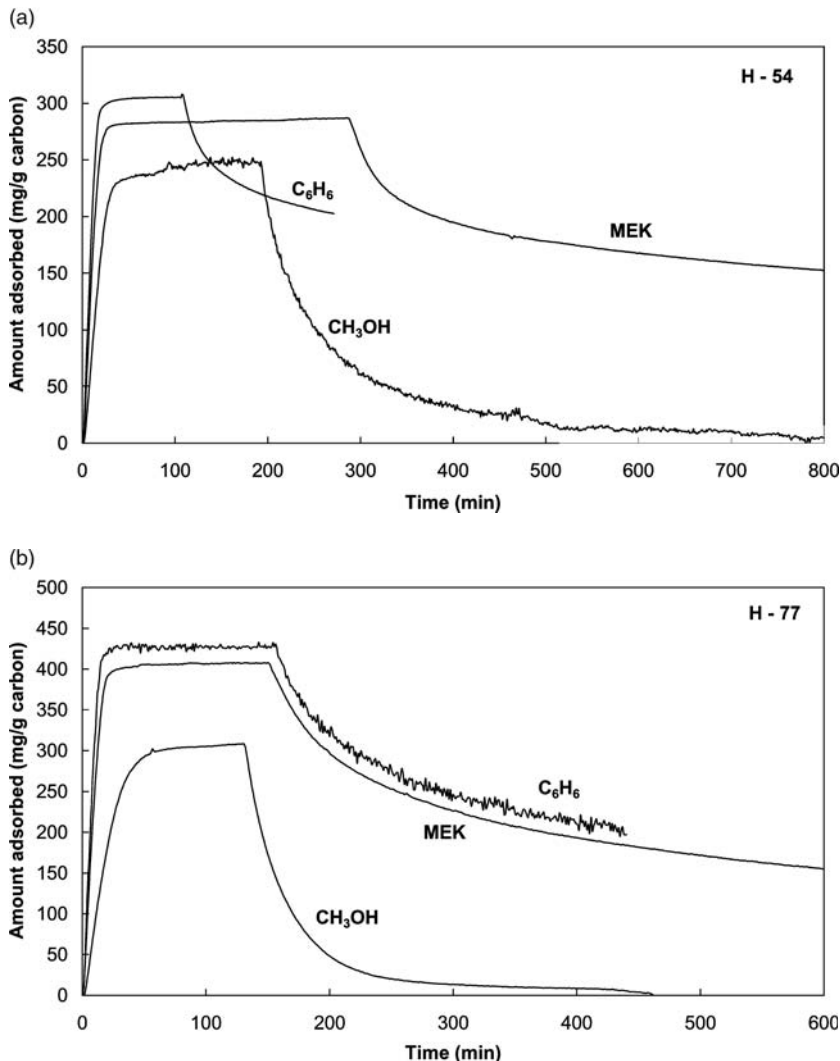


**Figure 11.** Amount of benzene, MEK and methanol adsorbed on H-54 (a) and on H-77 (b) activated carbons during the adsorption/desorption cycles as a function of time at 293 K and 0.2 relative pressures (benzene, MEK and methanol partial pressures of 2.06, 2.18 and 2.53 kPa, respectively).

water vapor molecules. This suggests that methanol molecules adsorbs initially in the most energetically and favorable adsorption sites. Only when all the adsorption centers of the activated carbon surface are occupied, methanol molecules are adsorbed through dispersive interactions. The change in the adsorption mechanism seems to be the cause of the lower adsorption rates exhibited by the polar organic vapors.

Previous studies focusing on MEK adsorption on activated carbon (23, 30, 57) have shown that the surface chemistry of the activated carbon plays an important role in the adsorption process, the amount of MEK adsorbed increasing with the presence of active centers. Nevertheless, adsorption of MEK on the activated carbons studied in this work appears to be very similar to that of benzene, a non-polar VOC.

The effect of the presence of water vapor on the benzene, MEK and methanol adsorption on H-77 carbon is illustrated in Fig. 12. The total amount adsorbed is higher for the mixture streams than for the cases where the streams contain only the VOC. However, it is underlined that the increase of the amount adsorbed in the case of the methanol/water vapor mixtures is much higher (from approximately 300 mg/g to more than 800 mg/g) than for both MEK and benzene water vapor mixtures (from approximately 400 mg/g to almost 600 mg/g). Methanol presents the highest solubility in water, while MEK has a solubility of 24% in water and benzene is almost insoluble in water, all at 293 K. It is also noteworthy the opening of the knee of the adsorption curves with VOC polarity (water solubility); while benzene/water mixture reaches the plateau zone sharply, methanol/water mixture does it very softly. Taqvi et al. (66) concluded that the ability of methanol to form hydrogen bonds with water molecules results in enhanced water adsorption and also enhanced methanol adsorption. Linders et al. (32) also found that methanol and ethanol adsorb better in the presence of water and ascribed the increased adsorption to water that is acting as additional adsorption sites.

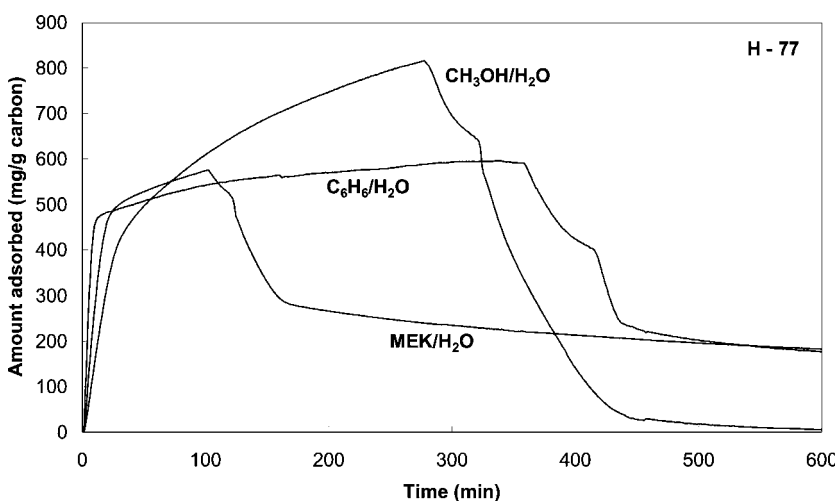


**Figure 12.** Amount adsorbed during adsorption/desorption cycles with inlet streams containing a benzene/water vapor, MEK/water vapor and methanol/water vapor (at 0.2 relative pressure for benzene, MEK and methanol and 0.8 relative pressure for water vapor) as a function of time on H-77 activated carbon at 293 K.

The desorption profile for MEK/water vapor mixture is quite similar to that for the benzene/water vapor mixture, indicating that the adsorbate is only partially desorbed at the adsorption temperature, with a significant amount of it remaining adsorbed on the carbon. This result suggests that, as in the case of benzene, MEK remains strongly adsorbed on the narrow micropores of the carbon. On the opposite, methanol/water vapor mixture is totally desorbed at the adsorption temperature.

## ACKNOWLEDGEMENTS

Financial support by the CICYT, through Project QUI97-0872, is gratefully acknowledged.

## REFERENCES

1. Khan, F.I. and Ghoshal, A., Jr. (2000) Removal of volatile organic compounds from polluted air. *Journal of Loss Prevention in the Process Industries*, 13 (6): 527–545.
2. Moretti, E.C. (2002) Reduce VOC and HAP emissions. *Chem. Eng. Progress*, 98: 30–40.
3. Gupta, V.K. (2002) Removal of volatile organic compounds by cryogenic condensation followed by adsorption. *Verma, N. Chem Eng. Sci.*, 57 (14): 2697–2705.
4. Ramanathan, K., Debler, V., Kosusko, M., and Sparks, L. (1998) Evaluation of control strategies for volatile organic compounds in indoor air. *Environ. Progress*, 7 (4): 230–235.
5. US EPA, Office of Research and Development. Soil vapor extraction technology reference handbook. Risk Reduction Engineering Laboratory. Report EPA/540/2-91-003, 1991.
6. US EPA, Pacific Environment Services, Inc. Soil vapor extraction VOC control technology assessment. Report EPA/450/4-89-017, 1989.
7. US EPA, Office of Solid Waste and Emergency Response. Analysis of selected enhancements for soil vapor extraction. Report EPA-542-R-97-007, 1997.
8. US EPA, Office of Solid Waste and Emergency Response. A citizen's guide to soil vapor extraction. Report EPA 542-F-96-008, 1996.
9. Marks, J.R. and Rhoads, T. (1991) Planning save time and money when installing VOC controls. *Chem. Proc.*, 5: 42.
10. Everaert, K. and Baeyens, J. (2004) Catalytic combustion of volatile organic compounds. *Journal of Hazardous Materials*, 109: 113–139.
11. Matros, Y.S., Noskov, A.S., and Chumachenko, V.A. (1993) Progress in reverse-process application to catalytic incineration problem. *Chem. Eng. Progr.*, 32: 89.
12. Van de Beld, B., Borman, A.A., Derkx, O.R., Van Woeliz, B.A., and Weserterp, K.R. (1994) Removal of VOC from polluted air in a reverse flow reactor. *Ind. Eng. Chem. Res.*, 33 (12): 2946–2956.
13. Kiared, K., Bieau, L., Brzezinski, R., Viel, J., and Heitz, M. (1996) Biological elimination of VOCs in bio-filter. *Environ. Progr.*, 15 (3): 148–152.
14. Ruddy, E.N. and Carroll, L.A. (1993) Select the best VOC control strategy. *Chem. Eng. Progr.*, 89 (7): 28–35.

15. Yun, J.H., Choi, D.K., and Kim, S.H. (1998) Adsorption of organic solvent vapors on hydrophobic Y-type zeolite. *AIChE J.*, 44 (6): 1344–1350.
16. Hu, X., Qiao, S., Zhao, X.S., and Lu, G.Q. (2001) Adsorption study of benzene in ink-bottle-like MCM-41. *Ind. Eng. Chem. Res.*, 40: 862–867.
17. Zhao, X.S., Ma, Q., and Lu, G.Q. (1998) VOC removal: comparison of MCM-41 with hydrophobic zeolites and activated carbon. *Energy & Fuels*, 12: 1051–1054.
18. Yun, J.H., Choi, D.K., and Kim, S.H. (1998) Adsorption equilibria of chlorinated organic solvents onto activated carbon. *Ind. Eng. Chem. Res.*, 37 (4): 1422–1427.
19. Yun, J.H., Choi, D.K., and Kim, S.H. (1999) Equilibria and dynamics for mixed vapors of BTX in activated carbon bed. *AIChE J.*, 45 (4): 751–760.
20. Cal, M.P., Rood, M.J., and Larson, S.M. (1997) Gas phase adsorption of volatile organic compounds and water on activated carbon cloth. *Energy Fuels*, 11 (2): 311–315.
21. Dimotakis, E.D., Cal, M.P., Economy, J., Rood, M.J., and Larson, S.M. (1995) Chemically treated activated carbon cloth for removal of volatile organic carbons from gas stream: Evidence for enhanced physical adsorption. *Environ. Sci. Technol.*, 29 (7): 1876–1880.
22. Chiang, Y.C., Chiang, P.C., and Huang, C.P. (2001) Effects of pore structure and temperature on VOC adsorption on activated carbon. *Carbon*, 39: 523–534.
23. Chiang, Y.C., Huang, C.P., and Chiang, P.C. (2002) The adsorption of benzene and methylethylketone onto activated carbon: thermodynamic aspects. *Chemosphere*, 46: 143–152.
24. Lillo-Ródenas, M.A., Carratalá-Abril, J., Cazorla-Amorós, D., and Linares-Solano, A. (2002) Usefulness of chemically activated anthracite for the abatement of VOC at low concentrations. *Fuel Proc. Technol.*, 77–78: 331–336.
25. Wijmans, J.G. and Helm, V.D. (1989) A membrane system for separation and recovery of organic vapors from gas streams. *AIChE Symposium Series*, AIChE: New York; Vol. 272, 8574.
26. Paul, H., Philipen, C., Gerner, F.J., and Strathmann, H.J. (1988) Removal of organic vapor from air by selective membrane permeation. *Mem. Sci.*, 36: 363–372.
27. Huang, M.C., Chou, C.H., and Teng, H. (2002) Pore-size effects on activated carbon capacities for volatile organic compound adsorption. *AIChE J.*, 48 (8): 1804–1810.
28. Magnun, C.L., Daley, M.A., Braatz, R.D., and Economy, J. (1998) Effect of pore size of hydrocarbons in phenolic-based activated carbon fibers. *Carbon*, 36: 123–131.
29. Chiang, H.L., Huang, C.P., Chiang, P.C., and You, J.H. (1999) Effect of metal additives on physico-chemical characteristics of activated carbon exemplified by benzene and acetic acid adsorption. *Carbon*, 37: 1919–1928.
30. Chiang, H.L., Chiang, P.C., and Huang, C.P. (2002) Ozonation of activated carbon and its effects on the adsorption of VOCs exemplified by methylethylketone and benzene. *Chemosphere*, 47: 267–275.
31. Chiang, Y.C., Chiang, P.C., and Chang, E.E. (2001) Effects of surface characteristics of activated carbons on VOC adsorption. *J. Environ. Eng. (ASCE)*, 127 (1): 54–62.
32. Linders, M.J.G., Van Den Broeke, L.J.P., Kapteijn, F., Moulijn, J.A., and Van Bokhoven, J.J.G.M. (2001) Binary adsorption equilibrium of organics and water on activated carbon. *AIChE J.*, 47 (8): 1885–1892.
33. Cal, M.P., Rood, M.J., and Larson, S.M. (1996) Removal of VOCs from humidified gas streams using activated carbon cloth. *Gas. Sep. Purif.*, 10: 117–121.

34. Qi, S., Hay, K.J., and Cal, M.P. (2001) Predicting humidity effect on adsorption capacity of activated carbon fro water immiscible organic vapors. *Adv. Environ. Res.*, 4: 357–362.
35. Dreisbach, F., Lösch, H.W., and Nakai, K. (2001) Adsorption measurements of water/ethanol mixtures on activated carbon fiber. *Chem. Eng. Technol.*, 24: 1001–1005.
36. Heinen, A.W., Peters, J.A., and Van Bekkum, H. (2000) Competitive adsorption of water and toluene on modified activated carbons supports. *Appl. Catal. A*, 194–195: 193–202.
37. Dubinin, M.M. and Serpinsky, V. (1981) Isotherm equation for water adsorption by microporous carbonaceus adsorbents. *Carbon*, 19 (5): 402–403.
38. Dubinin, M.M. (1980) Water vapor adsorption and the microporous structures of carbonaceus adsorbents. *Carbon*, 18: 355–364.
39. Brennan, J.K., Bandosz, T.J., Thomson, K.T., and Gubbins, K.E. (2001) Water in porous carbons. *Colloids and Surface A*, 187–188: 539–568.
40. McCallum, C.L., Bandosz, T.J., McGrother, C., Müller, E.A., and Gubbins, K.E. (1999) A molecular model for adsorption of water on activated carbon: comparison of simulation and experiment. *Langmuir*, 15: 533–544.
41. Do, D.D. and Do, H.D. (2000) A model for water adsorption in activated carbon. *Carbon*, 38 (5): 767–773.
42. Salame, I.I. and Bandosz, T.J. (1999) Experimental study of water adsorption on activated carbons. *Langmuir*, 15: 587–593.
43. Lee, W.H. and Reucroft, P.J. (1999) Vapor adsorption on coal- and wood- based chemically activated carbons (I) Surface oxidation states and adsorption of  $\text{H}_2\text{O}$ . *Carbon*, 37: 7–14.
44. Barton, S.S., Evans, M.J.B., and MacDonald, J.A.F. (1991) The adsorption of water by porous carbon. *Carbon*, 29 (8): 1099–1105.
45. Rodríguez-Mirasol, J., Cordero, T., and Rodríguez, J.J. (1993) Activated carbons from  $\text{CO}_2$  partial gasification of Eucalyptus kraft lignin. *Energy Fuels*, 7: 133–138.
46. Rodríguez-Mirasol, J., Cordero, T., and Rodríguez, J.J. (1993) Preparation and characterization of activated carbons from eucalyptus kraft lignin. *Carbon*, 31: 87–95.
47. González-Serrano, E., Cordero, T., Rodríguez-Mirasol, J., and Rodríguez, J.J. (1997) Developoment of porosity upon chemical activation of kraft lignin with  $\text{ZnCl}_2$ . *Ind. Eng. Chem. Res.*, 36: 4832–4838.
48. Moreno-Castilla, C., Rivera-Utrilla, J., Carrasco-Marín, F., and López-Ramón, M.V. (1997) On the carbon dioxide and benzene adsorption on activated carbons to study their micropore structure. *Langmuir*, 13: 5208–5210.
49. Dubinin, M.M. (1989) Fundamentals of the theory of adsorption in micropores of carbon adsorbents: characteristics of their adsorption properties and microporous structures. *Carbon*, 27 (3): 457–467.
50. Bering, B.P., Dubinin, M.M., and Serpinski, V.V. (1972) On thermodynamics of adsorption in micropores. *J. Colloid Interface Sci.*, 38 (1): 185–194.
51. Dubinin, M.M. (1966) *Chemistry and Physics of Carbon*; Walker, P.L., ed.; Marcel Dekker: New York; Vol. 2, 51–120.
52. Stoeckli, F. (1998) Recent developments in Dubinin's theory. *Carbon*, 36 (4): 363–368.
53. Bansal, R.C., Donnet, J.B., and Stoeckli, H.F. (1988) *Active Carbon*; Marcel Dekker: New York.

54. Terzyk, A.P., Gauden, P.A., and Kowalczyk, P. (2002) What kind of pore size is assumed in the Dubinin-Astakhov adsorption isotherm equation? *Carbon*, 40: 2879–2886.
55. Linders, M.J.G., van den Broeke, L.J.P., Nijhuis, T.A., Kapteijn, F., and Moulijn, J.A. (2001) Modelling sorption and diffusion in activated carbon: a novel low pressure pulse-response technique. *Carbon*, 39 (14): 2113–2130.
56. Linders, M.J.G. (1999) Prediction of breakthrough curves of activated carbon based sorption systems; from elementary steps to process design. Delft University of Technology, PhD. Thesis.
57. Huand, Z.H., Kang, F., Zheng, Y.P., Yang, J.B., and Liang, K.M. (2002) Adsorption of trace polar methyl-ethyl-ketone and non-polar benzene vapors on viscose rayon-based activated carbon fibres. *Carbon*, 40: 1363–1367.
58. Stoeckli, F. (2002) Water adsorption in activated carbons of various degrees of oxidation described by the Dubinin equation. *Carbon*, 40: 969–971.
59. Alcañiz-Monge, J., Linares-Solano, A., and Rand, B. (2001) Water adsorption on activated carbons: Study of water adsorption in micro- and mesopores. *J. Phys. Chem. B*, 105 (33): 7998–8006.
60. Chagger, H.K., Ndaji, F.E., Sykes, M.L., and Thomas, K.M. (1995) Kinetics of adsorption and diffusional characteristics of carbon molecular sieves. *Carbon*, 33 (10): 1405–1411.
61. Pedrero, C., Cordero, T., Rodríguez-Mirasol, J., and Rodríguez, J.J. (2001) Preparation of carbon molecular sieves by chemical vapor infiltration of lignin based microporous carbons, Proceedings of Carbon 2001, Lexington, Kentucky.
62. Rosas, J.M., Bedia, J., Rodríguez-Mirasol, J., and Cordero, T. (2003) Kinetics of pyrolytic carbon infiltration for the preparation of ceramic/carbon and carbon/carbon composites, Proceedings of Carbon 2003, Oviedo, Spain.
63. Pedrero, C., Cordero, T., Rodríguez-Mirasol, J., and Rodríguez, J.J. (2002) Preparation of characterization of carbon molecular sieves obtained by high temperature treatment of lignin, Proceedings of Characterization of Porous Solids VI, Alicante, Spain.
64. Salame, I.I. and Bandosz, T.J. (2000) Adsorption of water and methanol on micro- and mesoporous wood-based activated carbons. *Langmuir*, 16: 5435–5440.
65. Bandosz, T.J., Jagiello, J., Schwarz, J., and Krzyzanowski, A. (1996) Effect of surface chemistry on sorption of water and methanol on activated carbons. *Langmuir*, 12: 6480–6486.
66. Taqvi, S.M., Appel, W.S., and Le Van, M.D. (1999) Coadsorption of organic compounds and water vapour on BPL activated carbon. 4. Methanol, ethanol, propanol, butanol and modelling. *Ind. Eng. Chem. Res.*, 38 (1): 240–250.